



Trade Science Inc.

Materials Science

An Indian Journal

Full Paper

MSAIJ, 2(6), 2006 [229-233]

Evaluation Of Crystallization Kinetics Of $\text{Fe}_{85}\text{Zr}_{3.5}\text{Nb}_{3.5}\text{B}_7\text{Cu}_1$ Amorphous Alloy By Non-Isothermal Analysis

Corresponding Author

Kun Peng^{1,2}

¹College of materials Science and Engineering, Hunan University, Changsha, 410082, (CHINA)

²State Key Laboratory of Powder Metallurgy, Central South University, Changsha 410083, (CHINA)

E-mail: kpeng@hnu.cn

Received: 14th November, 2006Accepted: 29th November, 2006Web Publication Date : 27th December, 2006

Co-Authors

LingPing Zhou¹, Dingfa Fu¹, AiPing Hu¹, Feng Xu³

¹College of materials Science and Engineering, Hunan University, Changsha, 410082, (CHINA)

³Department of Materials Science and Engineering, Nanjing University of Science and Technology, Nanjing-210094, (CHINA)

ABSTRACT

The crystallization processes for the amorphous $\text{Fe}_{85}\text{Zr}_{3.5}\text{Nb}_{3.5}\text{B}_7\text{Cu}_1$ alloy were investigated using no-isothermal method. The crystallization data are analyzed in terms of a modified Kissinger's equation to determine the activation energy (E) and the Avrami exponent (n). The obtained activation energies for the first crystallization is $271 \pm 19 \text{ kJ/mol}$, with the crystallization kinetics proceeding by a three-dimensional diffusion controlled grain growth on pre-existing nuclei, where $n=1.3$. And the obtained activation energies for the second crystallization is $466 \pm 7 \text{ kJ/mol}$ and where $n=2.0$, with the crystallization kinetics proceeding by a three-dimensional diffusion controlled grain growth of small particles with decreasing nucleation rate.

© 2006 Trade Science Inc. - INDIA

INTRODUCTION

The nanometer scale crystalline structure in NANOPERM alloys is responsible for their soft magnetic properties. The soft magnetic properties are closely dependent on the microstructure. And this

nanocrystalline structure is obtained by partially crystallization of the amorphous precursor. The understanding of the crystallization kinetics of magnetic amorphous alloys has two important reasons. First, for the case of an alloy that exhibits good magnetic properties in its amorphous phase, the crystalliza-

Full Paper

tion kinetics represents the limit at which the properties begin to deteriorate, thus the thermal stability determines the magnetic stability of the amorphous phase of the materials. Second, for the case of an alloy that exhibits excellent magnetic properties in the two-phase nanocrystalline structures. Control the crystallization process allows the ability to tailor the microstructure and then obtain the desired magnetic properties. Therefore, the control of crystallization of amorphous is often critical for the preparation of desirable microstructures, and much attention has been paid to the mechanism of structural evolution. Thermal analysis method is widely used for kinetic analysis of crystallization processes in the amorphous solids^[1-7]. Two thermal analysis methods are available: one is the non-isothermal method^[1-4], in which amorphous samples are heated up at a constant heating rate; and the other is isothermal method^[5-7], in which amorphous samples are quickly heated up and held at a temperature above the glass transition temperature. In this method, amorphous samples crystallize at a constant temperature. Generally, an isothermal experiment takes longer time than a non-isothermal experiment, but isothermal experimental data can be interpreted by the well-established Johnson-Mehl-Avrami equation^[5-7]. On the contrary, non-isothermal experiments themselves are rather simple and quick, but assumptions are usually required for data interpretation because there is no uniquely accepted equation available for non-isothermal method. Several equations for interpreting non-isothermal data have been proposed and used^[1-4].

Theoretical analysis

The crystallization kinetic during the isothermal treatment process, the time evolution of crystalline volume fraction, x , can be described by the Johnson-Mehl-Avrami equation as^[8-10].

$$x = 1 - \exp[-(Kt)^n] \quad (1)$$

Where n is the Avrami exponent and K is the reaction rate constant, which is associated with the activation energy (which describes the overall crystallization process, nucleation and growth, for a single reaction), E , and the frequency K_0 through the Arrhenius temperature dependence,

$$K = K_0 \exp(-E/RT) \quad (2)$$

where T is absolute temperature, R is the gas constant.

Applying the JMA equation to the non-isothermal transition of glasses needs to take into account to the dependence of K on time, t , thus,

$$x = 1 - \exp\left[-\left(\int_0^t K(t)dt\right)^n\right] \quad (3)$$

At a certain temperature, T_p , when

$$\frac{d^2x}{dt^2}\bigg|_{T=T_p} = 0 \quad (4)$$

the crystallization rate of the amorphous dx/dt reaches its maximum. By taking the second derivative of equation (3) and combining with equation (4), one can finally derive an equation relating the crystallization kinetics parameters of the amorphous alloys to the temperature T_p and the heating rate b . In the case of non-isothermal, it can be shown that a generalization of the JMA theory leads to the validation of the Kissinger analysis, through the equations^[11-13].

$$\ln(T_p^2/\beta) = E/RT_p - \ln(K_0R/E) \quad (5)$$

$$n = \left(\frac{dx}{dt}\right)_p RT_p^2 [E\beta(1-x_p)]^{-1} \quad (6)$$

where β is the constant heating rate and p refers to the variables at maximum crystallization rate. It is possible to obtain both the overall effective activation energy and the frequency factor of the crystallization process. It is obviously that the plot of $\ln(T_p^2/\beta)$ versus $1/T_p$ should be linear and the activation energy, E , can be easily determined from the slope. When $E \gg RT_p$ and the crystallization fraction for the maximum crystallization rate is 0.63, which is independent of the heating rate and of the Avrami exponent^[12], then equation (6) can be transferred into the form^[14,15].

$$n = \left(\frac{dx}{dt}\right)_p RT_p^2 (0.37\beta E)^{-1} \quad (7)$$

which make it possible to calculate the kinetic exponent n .

EXPERIMENTAL

Amorphous ribbons of $\text{Fe}_{85}\text{Zr}_{3.5}\text{Nb}_{3.5}\text{B}_7\text{Cu}_1$ alloy

were prepared by single-roller spinning method. The obtained ribbons are about 25 μm in thickness and 1 mm in width, showing no evidence of crystallization in the X-ray diffraction patterns. The crystallization behaviors of the amorphous alloys were studied by means of differential thermal analyzer (DTA). The non-isothermal experiments were performed in Perkin-Elmer DSC-7 differential Scanning Calorimeter under Ar atmosphere with a heating rate of 5, 10, 15 and 20 K/min, each sample was heated from 473K to 1173K, the peak crystallization temperature (T_p) was determined from DTA curves.

RESULTS AND DISCUSSION

Figure 1 shows the DTA curves of the amorphous $\text{Fe}_{85}\text{Zr}_{3.5}\text{Nb}_{3.5}\text{B}_7\text{Cu}_1$ alloy at different heating rate. Where it is observed that this alloy has two stages crystallization for all the applied heating rates. It was shown that the peak temperature increase as the heating rates increase, suggesting a dependence of peak temperature on the heating rate of the sample. The XRD patterns indicates that the first crystallization step corresponds to the formation of $\alpha\text{-Fe}$ phase and the second one corresponds to the formation of the Fe_3B phase (seen in figure 2). It is in accordance with other author's results the first peak corresponds to the formation of $\alpha\text{-Fe}$ phase, and the second peak is associated to the crystallization of the residual amorphous phase, it is also explained

the formation of Fe-borides^[16-18]. It is apparently that the peak temperature T_p increase with increasing heating rate, the area under the DTA curve is directly proportional to the total amount of alloy crystallized. Both of the crystallization kinetic parameters for the formation of both of $\alpha\text{-Fe}$ phase and Fe_3B phase in $\text{Fe}_{85}\text{Zr}_{3.5}\text{Nb}_{3.5}\text{B}_7\text{Cu}_1$ alloy were investigated.

If T_p^2/β is measured in a series of exothermal reaction taken at different heating rates, the plot of $\ln(T_p^2/\beta)$ as a function of $1/T_p$ should be a linear function with the slope of E/R . The $\ln(T_p^2/\beta)$ versus $1/T_p$ curves for $\text{Fe}_{85}\text{Zr}_{3.5}\text{Nb}_{3.5}\text{B}_7\text{Cu}_1$ alloy are shown in figure 3, then the activation energy E can be obtained, $E_1=271\pm 19\text{kJ/mol}$ and $E_2=466\pm 7\text{kJ/mol}$, where the subscript 1 and 2 refer to the first and the second crystallization process respectively. The activation energy for Fe self-diffusion in pure BCC $\alpha\text{-Fe}$ is 239.7kJ/mol at atmospheric pressure^[19]. However, it can be seen from the experimentally determined higher values of activation energy that Zr, Nb and B also play a part in the crystallization of NANOPERM. The densities of Zr, Nb and B are lower in the $\alpha\text{-Fe}$ region and higher in the amorphous phase^[20], the Zr, Nb and B diffuses away from the growing crystals. Therefore, the activation energy in $\text{Fe}_{85}\text{Zr}_{3.5}\text{Nb}_{3.5}\text{B}_7\text{Cu}_1$ alloy is higher than that in pure Fe. And the value of activation energy in

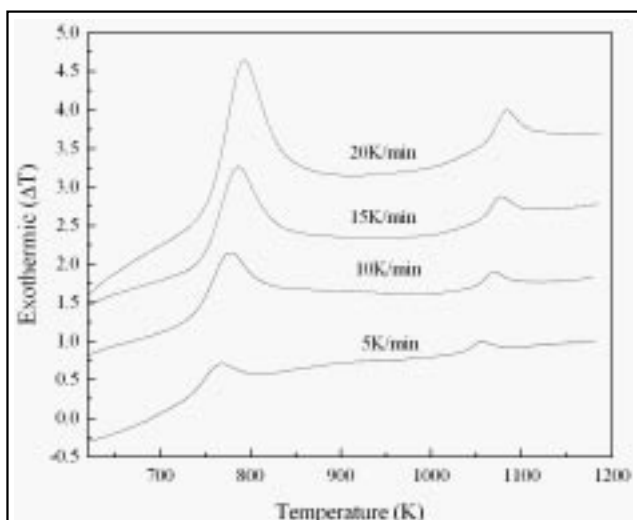


Figure 1: DTA curves obtained at different heating rates for $\text{Fe}_{85}\text{Zr}_{3.5}\text{Nb}_{3.5}\text{B}_7\text{Cu}_1$ amorphous alloy

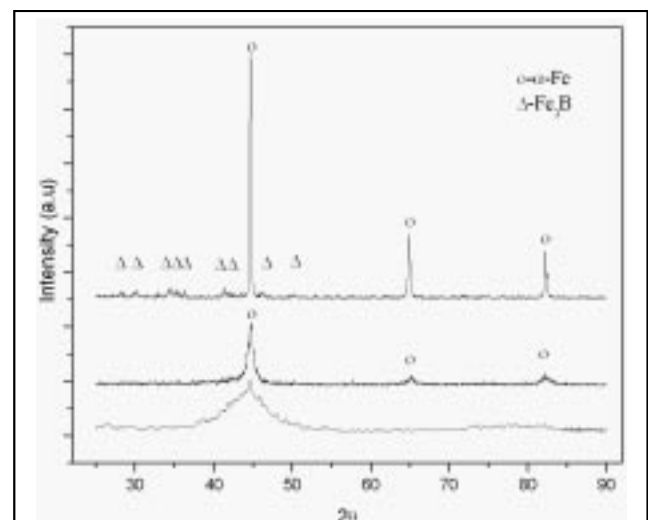


Figure 2: XRD data for spun and the sample annealed at 823K and 1073K for 1 hour

Full Paper

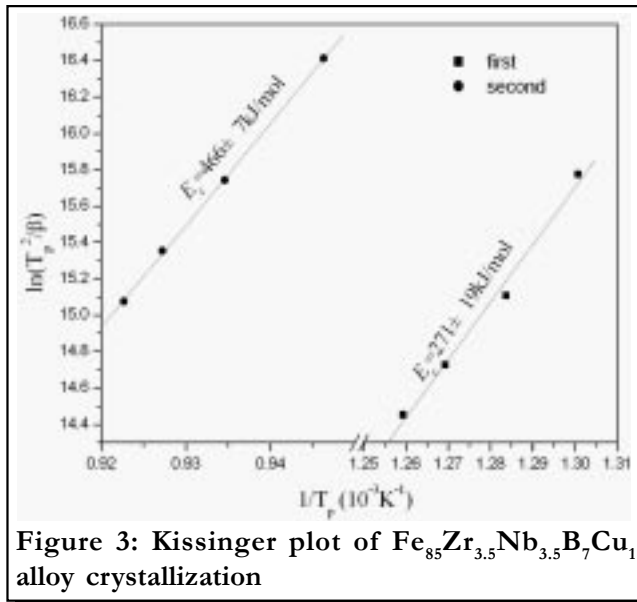


Figure 3: Kissinger plot of $\text{Fe}_{85}\text{Zr}_{3.5}\text{Nb}_{3.5}\text{B}_7\text{Cu}_1$ alloy crystallization

$\text{Fe}_{85}\text{Zr}_{3.5}\text{Nb}_{3.5}\text{B}_7\text{Cu}_1$ alloy is a little smaller than those published in the literature on similar amorphous magnetic alloys (2.8–3.4 eV)^[21], which is due to the influence of alloy's composition. According to equation (5), it is also possible to obtain the frequency factor (K_0) of the crystallization process, the obtained K_0 are 3.9×10^{15} and 4.7×10^{20} for the first and the second crystallization in the $\text{Fe}_{85}\text{Zr}_{3.5}\text{Nb}_{3.5}\text{B}_7\text{Cu}_1$ amorphous alloy respectively.

The area under the DTA curve is proportional to the total amount of alloy crystallized. The crystallized fraction, x , at any temperature T is given as $x = A_T/A$, where A is the total area of the exothermal between the onset temperature T_i , where the crystallization is just beginning and the temperature T_p where the crystallization is completed and A_T is the area between the onset temperature T_i and any given temperature T . The ratio between the ordinates and the total area of the peak gives the corresponding crystallization rates, which make it possible to plot the curves of the exothermal peaks represented in figure 4. It was observed that the $(dx/dt)_p$ values increase in the same proportion as the heating rates increase; a property has been discussed in the literature^[22]. In addition, the experimental data of T_p and $(dx/dt)_p$, which correspond to the maximum crystallization rate for each heating rate. Then equation (6) and (7) can be used to determine the Avrami exponent, n , as an average of the set of parameters obtained for different heating rates.

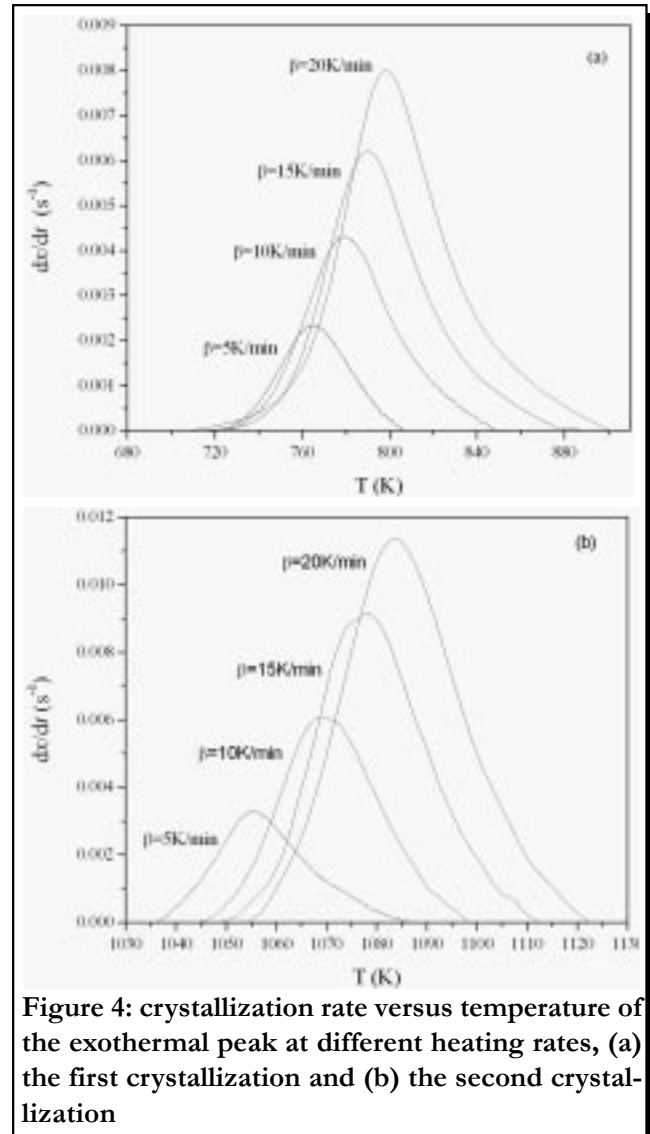


Figure 4: crystallization rate versus temperature of the exothermal peak at different heating rates, (a) the first crystallization and (b) the second crystallization

The obtained value of n of the first crystallization process is 1.3, which can be associated with a three-dimensional diffusion controlled grain growth on pre-existing nuclei^[23], which produced mainly during quench or prior to the primary crystallization. It was found that Cu clusters form prior to the onset of the primary crystallization by using atom probe field ion microscopy^[24]. More recently, it was investigated that the Cu clusters form prior to the onset of the primary crystallization and directly serve as heterogeneous nucleation sites for the α -Fe primary crystals^[20]. The obtained value of n of the second crystallization process is 2.0, which can be associated with a three-dimensional diffusion controlled grain growth with a decreasing nucleation rate^[23].

CONCLUSION

The crystallization processes for the amorphous $\text{Fe}_{85}\text{Zr}_{3.5}\text{Nb}_{3.5}\text{B}_7\text{Cu}_1$ alloy were investigated using non-isothermal method. The obtained activation energies are $271 \pm 19 \text{ kJ/mol}$ and $466 \pm 7 \text{ kJ/mol}$ for the formation of $\alpha\text{-Fe}$ and Fe_3B phase. The formation of $\alpha\text{-Fe}$ was associated with a three-dimensional diffusion controlled grain growth on pre-existing nuclei, and the formation of Fe_3B phase was associated with a three dimensional diffusion controlled grain growth with a decreasing nucleation rate.

ACKNOWLEDGEMENTS

This work was supported by National Natural Science Foundation of China (50501008) and Hunan Provincial Natural Science Foundation of China (04jj3010).

REFERENCE

- [1] Jiri Malek; *Thermochimica Acta*, **355**, 239 (2000).
- [2] Richa Agrawal, N.S.Saxena, K.B.Sharma, S.Thomas, M.S.Sreekala; *Mater.Sci.Eng.*, **A277**, 77 (2000).
- [3] Kangguo Cheng; *J.Mater.Science*, **36**, 1043 (2001).
- [4] N.P.Basal, R.H.Doremus; *J.Therm.Anal.*, **29**, 115 (1984).
- [5] D.G.Morris; *Acta Metall.Mater.*, **29**, 1213 (1981).
- [6] J.Q.Zhu, Z.L.Bo, D.K.Dong; *Phys.Chem.Glasses*, **37**, 264 (1996).
- [7] M.A.Hong, G.L.Messing; *J.Am.Ceram.Soc.*, **80**, 1551 (1997).
- [8] M.Avrami; *J.Chem.Phys.*, **7**, 1103 (1939).
- [9] W.A.Johnson, F.Mehl; *Trans.Am.Inst.Mining Met.Eng.*, **135**, 416 (1939).
- [10] M.Avarmi; *J.Chem.Phys.*, **9**, 177 (1941).
- [11] J.Vazquez, P.L.Lopez-Aleman, P.Villares, R.Jimenez-Garay; *J.Phys.Chem.Solids*, **61**, 493 (2000).
- [12] J.Vazquez, R.A.Ligero, P.Villares, R.Jimenez-Garay; *Thermochim.Acta*, **157**, 181 (1990).
- [13] P.L.Lopez-Aleman, J.Vazquez, P.Villares, R.Jimenez-Garay; *J.Non-Cryst.Solids*, **274**, 249 (2000).
- [14] D.S.dos Santos, D.R.dos Santos; *J.Non-Cryst.Solids*, **304**, 56 (2002).
- [15] P.L.Lopez-Aleman, J.Vazquez, P.Villares, R.Jimenez-Garay; *Mater.Chem.Phys.*, **65**, 150 (2000).
- [16] J.S.Garitaonandia, D.S.Schmool, J.M.Barandiaran; *Phys.Rev.*, **B58**, 12147 (1998).
- [17] A.Slawska-Waniewska, J.M.Greneche; *Phys.Rev.*, **B56**, R8491 (1997).
- [18] M.Miglierini, J.M.Greneche; *J.Phys.Condens.Mater.*, **9**, 2321 (1997).
- [19] M.Al-Haj, J.Barry; *J.Mater.Sci.Lett.*, **16**, 20, 1640 (1997).
- [20] T.Ohkubo, H.Kai, D.H.Ping, K.Hono, Y.Hirotsu; *Scripta Mater.*, **44**, 971 (2001).
- [21] A.Hsiao, M.E.Mchenry, D.E.Laughlin, M.J.Kramer, C.Ashe, T.Ohkubo; *IEEE Transactions on Magnetic*, **38**, 5, 3039 (2002).
- [22] J.Vazquez, P.L.Lopez-Aleman, P.Villares, R.Jimenez-Garay; *Mater.Chem.Phys.*, **57**, 162 (1998).
- [23] J.Christian; in 'The Theory of Transformations in Metals and Alloys', Pergamon, Oxford, 1542 (1975).
- [24] Y.Zhang, K.Hono, A.Inoue, T.Sakurai; *Mater.Sci.Eng.*, **A217/218**, 407 (1996).